# Sensors Technology (ELCT903)
# Capacitive Force Sensor

Ann Ezzat, Anthony Ussama, Joseph Maher, Paula Magdy, Salma Essam, Somayah Mansour

***Abstract*—This paper presents the comprehensive development and analysis of a capacitive-based force sensor utilizing ABS (Acrylonitrile Butadiene Styrene) material. The sensor's core principle lies in the conversion of physical changes induced by applied forces into measurable capacitance alterations within the sensor's circuitry. The sensitivity assessment revealed a sensitivity of 3 mV/N, indicating its ability to accurately measure force variations. Additionally, the sensor exhibited low hysteresis of 7.73%, with a resolution of 0.93 N and an operational range from 0.93 N to 6.8 N. The dynamic characteristics analysis categorized the sensor as a second-order system, step input, specifically identified as underdamped.**

## I. Introduction

The pursuit of precise and efficient force measurement techniques has driven the exploration and development of novel sensor technologies. Within this context, this report presents an in-depth exploration into the design, analysis, and practical implementation of a capacitive-based force sensor utilizing ABS (Acrylonitrile Butadiene Styrene) material.

The need for accurate force sensing finds applications across diverse fields, including robotics, biomechanics, and industrial automation, where the reliable measurement of forces is integral. The utilization of ABS material, known for its mechanical resilience and versatility, serves as the foundation for this sensor's construction, enabling the translation of applied forces into measurable output signals.

This milestone report delves into the comprehensive design flow, material considerations, theoretical analysis, and practical implementations involved in the development of the capacitive force sensor. The sensor's core principle lies in the conversion of physical changes induced by applied forces into measurable capacitance alterations within the sensor's circuitry.

Key elements such as the top, elastic, ring, and bottom elements contribute synergistically to the sensor's functionality. The report offers an intricate understanding of each component's role in the sensor's operation, elucidating the interplay between structural design and the sensor's force-sensing capabilities.

Moreover, theoretical simulations using Ansys Software have been conducted to ascertain the ABS elastic element's deflection concerning the material's yield strength. This exploration aims to ensure the sensor's operational safety margins by determining deflection limits under various force conditions.

In conjunction with theoretical analyses, practical assessments of force measurement techniques are outlined. The report details the methodology for measuring and confirming the initial natural frequency, followed by the application of forces and subsequent resonance frequency shifts. These shifts enable the derivation of force magnitudes applied to the sensor.

Additionally, Power amplification circuitry has been devised to augment the sensor's performance, integrating an Op-amp to linearize and amplify the sensor output.

## II. Designing Flow for Sensor

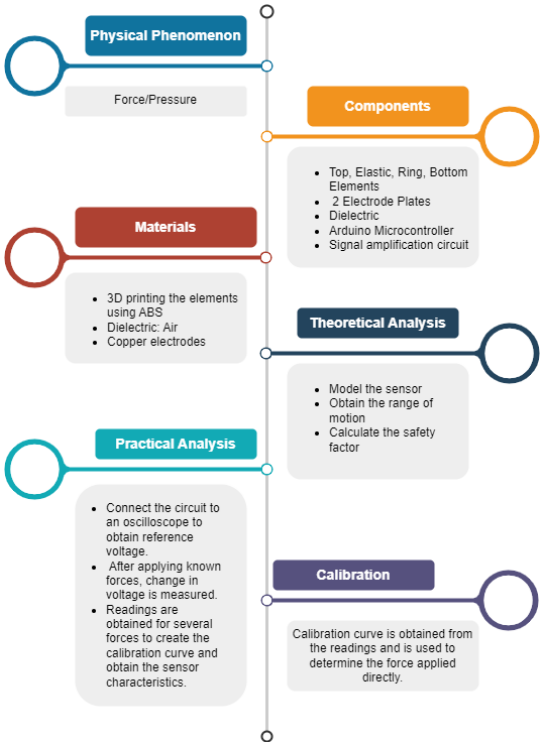


Fig. 1: Designing Flow for Sensor: Capacitive Force Sensor

## III. Components and Materials

In a capacitive-based force sensor, the ABS material undergoes a physical change under the applied force, which is then transformed into a measurable output signal by a capacitor. A schematic of the developed sensor is depicted in Figure 2. The sensor uses parallel-plate capacitors to measure normal force, and a vertical cylinder surrounding the sensor consisting of two parallel-plate capacitors to measure shear force. When the distance between two parallel plates of the capacitor changes, the capacitance of the capacitor also changes. The two parallel

plates used to measure the normal force are attached to the elastic element and a fixed bottom plate, respectively. The plate attached to the elastic element moves when the elastic element deforms in response to applied forces. Both the capacitance and the spacing between the parallel plates change as it moves. Figure 9 illustrates the designing flow for the capacitive force sensor using ABS material.

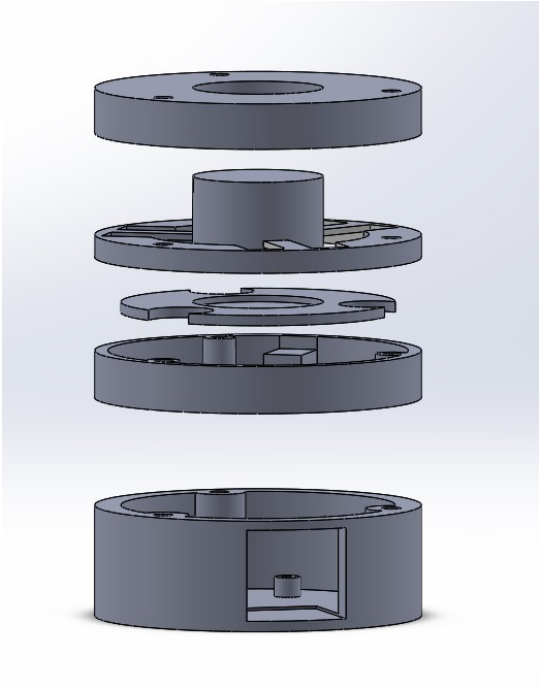

Fig. 2: Sensor Exploded View

- **Top element**: It serves as the upper enclosure of the sensor, featuring three M3 holes through which three nails are inserted to securely fasten all primary components of the sensor and to ensure that the force applied is only a normal force.
- **Elastic element**: The elastic element, featuring three cantilever beams connected to a solid cylinder, is designed to accommodate a maximum deformation of 2 mm. This deformation is achieved through the interplay of the three cantilever beams, complemented by stoppers integrated into the ring element, as illustrated in Figure 5. Additionally, these beams are linked to a substantial hollow cylinder, serving as a fixed support for the three beams.
- **Ring Element**: The ring element is equipped with M3 holes through which fixation nails are threaded. Additionally, it incorporates two stoppers strategically positioned to prevent the ground electrode from undergoing deformation beyond 2 mm.
- **Bottom Element**: The bottom element features M3 holes for the insertion of fixation nails. Additionally, it includes two cylinders with M2 holes, positioned at a height of 3 mm, to secure the lower PCB responsible for signal amplification. Above the lower PCB, a second PCB will be affixed at an elevation of 11 mm above the lower PCB, serving as the attachment point for the second electrode. The element also incorporates a dedicated slot for wiring.

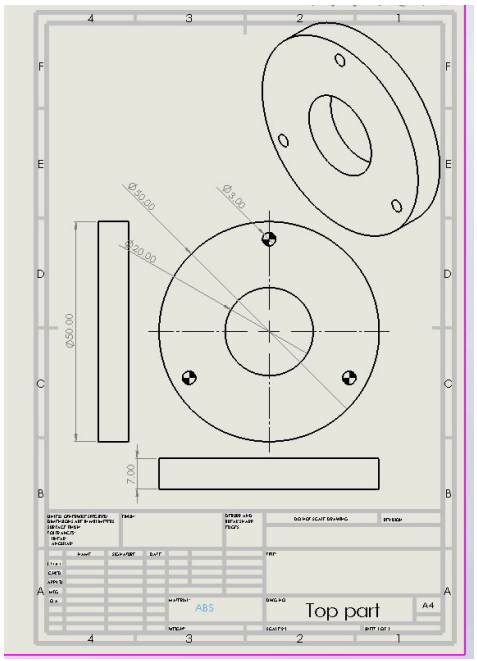


Fig. 3: Top Element

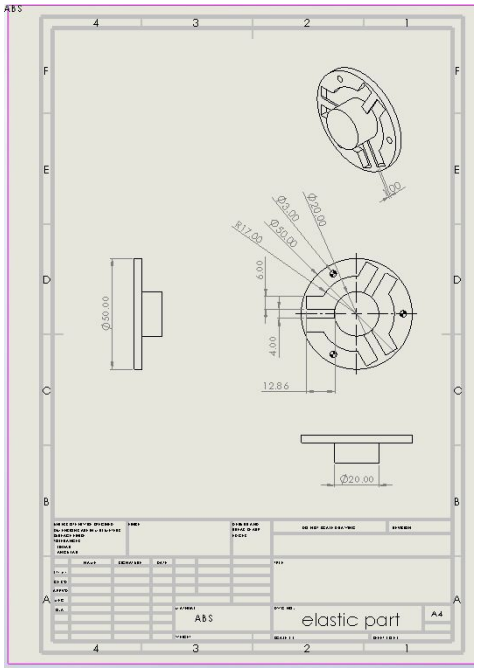


Fig. 4: Elastic Element

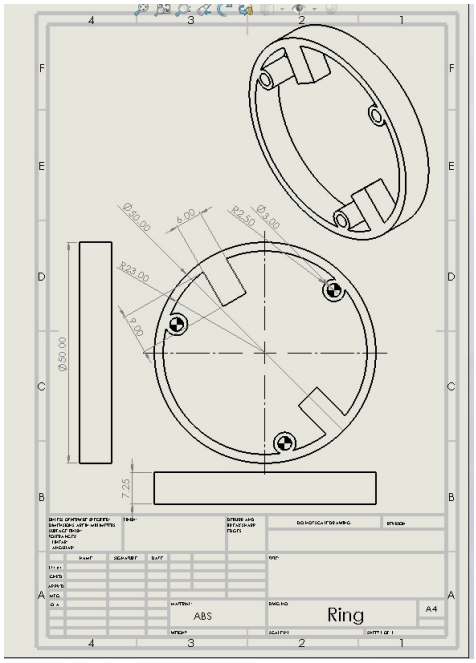


Fig. 5: Ring Element

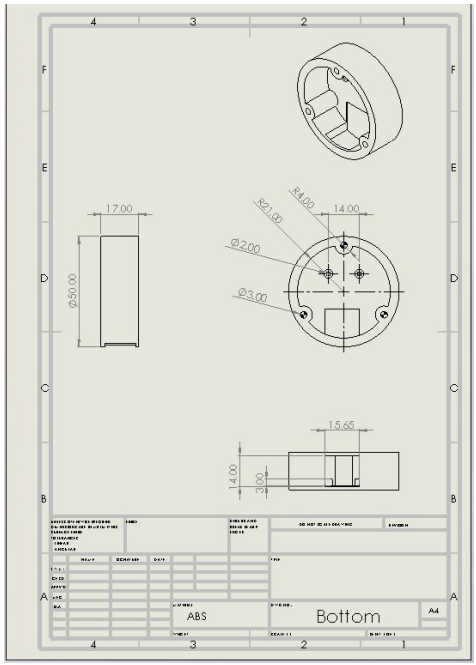


Fig. 6: Bottom Element

## IV. Theoretical Analysis

- **Simulation**:
  ANSYS Software was used to do the simulations on the ABS elastic element and determine the deflection that corresponds to the yield strength of ABS $\sigma_{max} = 40$ MPa and the safety factor in such case. As illustrated in the following figure, a total deformation of 1.9 mm is the maximum deflection achieved before the cantilever beams reach their yield point.

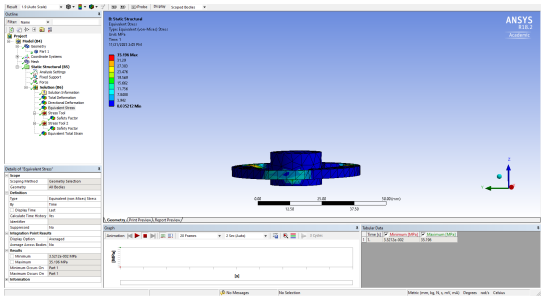

Fig. 7: Equivalent Stress = 35.196 MPa

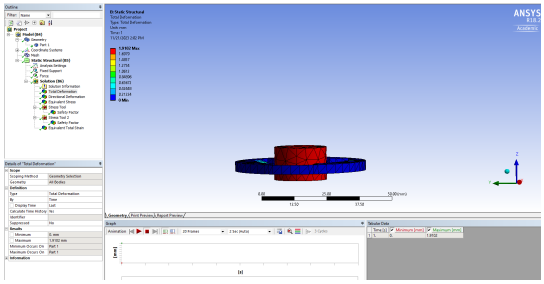

Fig. 8: Total Deformation = 1.9102 mm

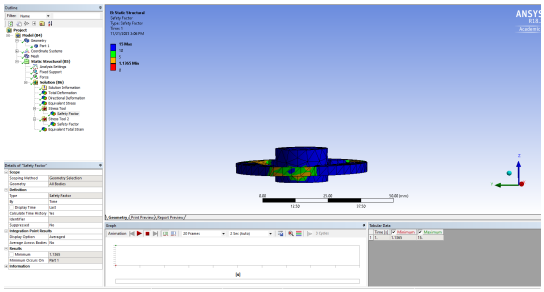

Fig. 9: Safety Factor = 1.1365

- **Calculations**
  To determine the maximum deflection when applying a stress equivalent to the yield stress equation 2 is used.

$$\frac{\delta_{\text{ymax}}}{\sigma_{\text{max}}} = \frac{2L^2}{3EH} \tag{1}$$

where:
$L$: Length of beam = 12 mm
$E$: Youngs Modulus of ABS material = 1.9 GPa

$H$: Height of beam = 1 mm
$\sigma_{\text{max}}$ : Yield Stress $= 40\,\text{MPa}$

After substituting with these values, it is obtained that the maximum deflection of a cantilever beam occurs at the end of the cantilever beam where $\delta_{\text{ymax}} = 2.02\,\text{mm}$. So, to prevent the structure from plastically deforming, stoppers are added to limit its motion to a maximum of 2 mm.

## V. Practical Analysis of Measuring the Applied Force

Once the sensor is securely housed, the circuit will be connected to an oscilloscope to measure and confirm the initial natural frequency without any exerted force. For this natural frequency, the initial capacitance is calculated and equivalently the initial separation between the capacitive plates using the following equation:

$$C = \varepsilon_0 \varepsilon_r \frac{A}{d} \tag{2}$$

where:
$C$: The capacitance of the two electrode plates ($C_0 =$ pF)
$\varepsilon_0$ : The dielectric constant of free space $= 8.85 \times 10^{-12}$ F/m
$\varepsilon_r$ : The dielectric constant of air $= 1.000569$
$d$: The distance between capacitive plates ($d_0 = 5.65\,\text{mm}$)
$A$: The area of the electrodes ($A_0 = 2698.67\,\text{mm}^2$)

To obtain a safe electric field of 250 V/m, according to the maximum deflection of 2mm, the minimum distance between 2 plates is 3.65mm, hence according to equation 3 a maximum voltage of 0.91V can be used across the capacitive plates.

$$E = V/d \tag{3}$$

where:
$E$: Electric field
$V$: Voltage
$d$: Distance between capacitive plates

Known forces are applied and the corresponding voltage changes are recorded to obtain a calibration curve. The separation between the plates can be calculated using equation 4.

$$\Delta d = \frac{F d_0}{E A_0} \tag{4}$$

## VI. Linearization Using Op-Amp and Power Amplification Circuit

In the pursuit of system linearization, reliance was placed on a power amplification circuit incorporating the IRF Z44N transistor. The amplification circuit shown in figure 10 played a pivotal role in elevating the current supplied to the op-amp circuit, thereby contributing to the attainment of readings. A capacitor of $1pf$ was added in parallel to the sensor to increase sensitivity. Before integrating the power amplifier, the circuit experienced persistent issues, characterized by a lack of capacitance variation, an absence of current flow, and no output voltage. The incorporation of the power amplification circuit effectively addressed these challenges, culminating in the establishment of a more responsive and reliable system.

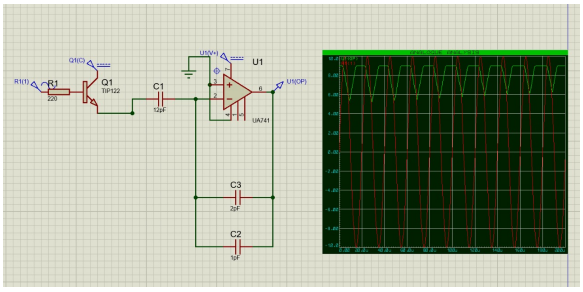


Fig. 10: Signal Linearization Circuit

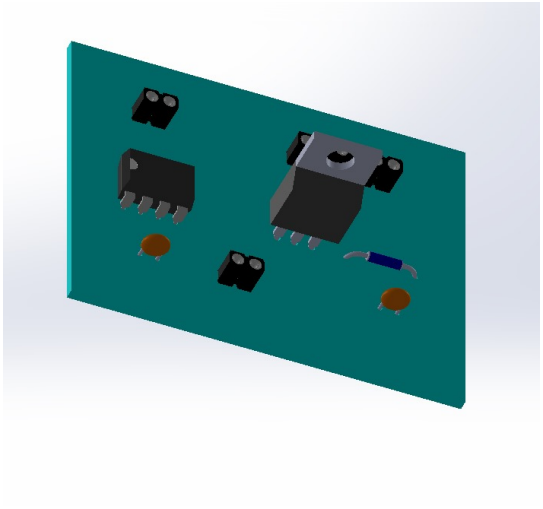

Fig. 11: PCB

## VII. Equation Of Motion

The Lagrangian approach is used to derive the equation governing the electromechanical system, ensuring that the behavior of the mechanical model is consistent with its electrical counterpart.

### A. Mechanical Model

In deriving the Lagrangian formulation, we incorporate the mass of the moving cylinder and the applied load (m), the spring constant of the cantilever beams (k), and the damping coefficient of the cantilever beams (b). The initial step involves calculating the kinetic energy in the following manner.

$$T = \frac{1}{2} m\dot{x}^2 \tag{5}$$

Subsequently, we compute the potential energy:

$$V = \frac{1}{2} kx^2 \tag{6}$$

The dissipation components arise from the damping coefficient :

$$D = \frac{1}{2} b\dot{x}^2 \tag{7}$$

Substituting in the lagrangian formulation given by:

$$m\ddot{x} + b\dot{x} + kx = f(t) \tag{8}$$

where f(t) is the acting force to be measured. Additionally, the remaining parameters are specified as follows: $m = 5.5\ grams$ + (external load). To determine the spring constant (k) and damping coefficient (b), ANSYS simulations were run to measure the displacement and velocity response when a step force was applied . When a force of 5N was used, the maximum deflection was found to be 0.42767 mm and the maximum velocity was 8.3962 mm/s. Given the following:

$$F = kx, \quad thus \quad k = \frac{F}{x} = 11.6\ N/mm \tag{9}$$

$$F = b\dot{x}, \quad thus \quad b = \frac{F}{x} = 0.6026\ Ns/mm \tag{10}$$

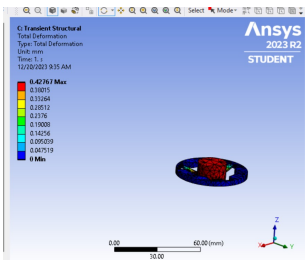


(a) Displacement Analysis

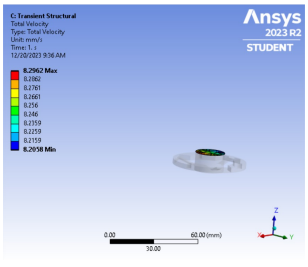


(b) Velocity Analysis

The natural frequency is $\sqrt{\frac{k}{m}}$ equals to 458.7 rad/s

### B. Electrical Model

With an initial capacitor displacement denoted as $x_0$ and the displacement caused by the applied force as $x$, and considering the linear relation deduced from the linearization circuit, the equation is as follows:

$$\frac{V_c}{V_{in}} = \frac{-C_f * d}{\epsilon * A} = \frac{-C_f(x - x_0)}{\epsilon * A} \tag{11}$$

Thus,

$$V_c = \frac{-V_{in} * C_f(x - x_0)}{\epsilon * A} \tag{12}$$

According to the equation $q = C * V_c$,

$$Q = (C1 + Cmeasured) * V_c \tag{13}$$

To establish the Lagrangian formulation, we begin by deriving the system's kinetic energy:

$$T = \frac{1}{2} L\dot{q}^2 \tag{14}$$

Since the L is very small, the kinetic energy is neglected for the ease of calculations.

Subsequently, we compute the potential energy according to equation 10 there are two capacitors connected in parallel:

$$V = \frac{1}{2}\frac{1}{C} q^2 = \frac{1}{2}\left[C1 + Cmeasuresd\right] V_c^2 \tag{15}$$

The dissipation components arise from the resistance value at the input and the output combined:

$$D = \frac{1}{2} R\dot{q}^2 = \frac{1}{2} R\left[C1 + Cmeasuresd^2\right] \dot{V_c}^2 \tag{16}$$

Substituting in the lagrangian formulation given by:

$$R\left[C1 + Cmeasuresd^2\right] \dot{V_c} + \left[C1 + Cmeasuresd\right] V_c = f(t) \tag{17}$$

where f(t) is the acting force to be measured. Additionally, the remaining parameters are specified as follows: $C1 = 1p$ F, resistance $R = 35.4Kohms$.

### C. Mechanical and Electrical Relation

Introducing a constant, let $K_1 = \frac{-V_{in} C_f}{\epsilon A}$. Hence, equation VII-B is restated as:

$$V_c = K_1 x - K_1 x_0 \tag{18}$$

As both $x = x_0 - \frac{V_c}{k_1}$ and $q = C * V_c$ are functions of $V_c$,

## VIII. Results

As it seen from 13 the output voltage is in phase with the input voltage although the circuit used in inverting circuit. This due to that the input frequency is 120 KHz while the natural frequency is 73 Hz. Since the frequency ratio is $r = \frac{w}{xn}$ so r is greater than one so there is 180 phase shift and this explains why the output is in phase with the input.

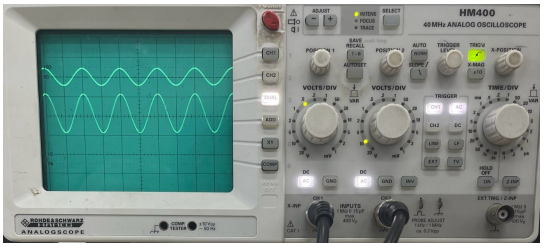


Fig. 13: Input voltage to the opamp and Output voltage from the opamp

### A. Calibration Curve Analysis

The calibration curve gets the correlation between output voltage and applied force on the sensor. Through subjecting the sensor to a spectrum of forces and recording the corresponding voltages,

*1) Sensitivity Assessment:* The sensitivity (S), discerned from the slope of the calibration curve, quantifies the sensor's responsiveness to variations in force. It is calculated as follows:

$$S = \frac{\Delta V}{\Delta F} \tag{19}$$

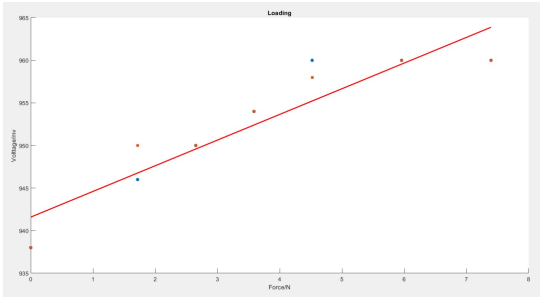


Fig. 14: Calibration Curve while loading

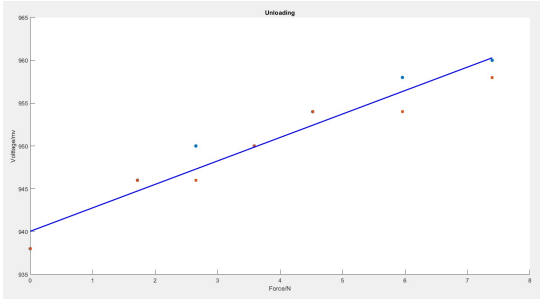


Fig. 15: Calibration Curve while unloading

In our specific case 14, the sensitivity is denoted by S = 3 mV/N.

*2) Hysteresis:* To assess hysteresis, the sensor underwent incremental and decremental force applications, with output voltages recorded. The hysteresis (H) is determined using the formula:

$$H = \frac{Y_{\text{mn}} - Y_{\text{mp}}}{Y_{\text{max}} - Y_{\text{min}}} \times 100\% \tag{20}$$

In our specific case , the hysteresis is denoted by H = 7.73%.

*3) Resolution and Range:* the resolution is 0.93 N. The operational range of the sensor is from 0.93 N to 6.8 N

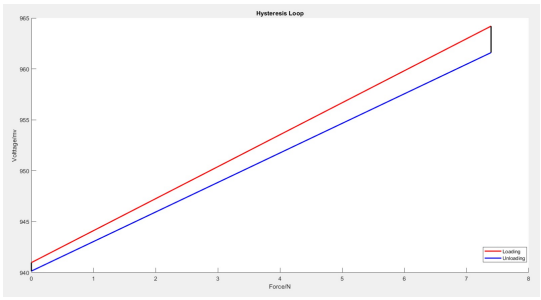


Fig. 16: Calibration Curves for Figures 14 and 15

### B. Dynamic Characteristics

The system being analyzed is categorized as a second-order system and is specifically identified as under-damped. To understand its behavior and performance under varying force conditions, a step input is applied to the system, and weights are placed on the force sensor to observe the corresponding output. This allows for a comprehensive exploration of the sensor's dynamic response and provides valuable insights. Based on the given values of natural frequency $\omega_n = 458.7$ rad/s , damping ratio $\zeta = \frac{b}{2\sqrt{km}} = 0.038$ and the damped frequency $\omega_d = \omega_n\sqrt{1-\zeta^2} = 458.36$ , we can derive several dynamic characteristics as follows :

- **Rise time:**

$$t_r = \frac{arctan(-\omega_d/\zeta)}{\omega_d} = 0.19sec \tag{21}$$

- **Maximum overshoot:**

$$M_p = exp(\frac{-\pi\zeta}{\sqrt{1-\zeta^2}}) = 0.887 \tag{22}$$

- **Peak time:**

$$t_p = \frac{\pi}{\omega_d} = 0.0068 \tag{23}$$

- **Resonance frequency:**

$$\omega_r = \omega_n\sqrt{1-2\zeta^2} = 457.7 \tag{24}$$

- **Resonance amplitude:**

$$M_r = \frac{1}{2\zeta\sqrt{1-\zeta^2}} = 13.167 \tag{25}$$

## IX. Conclusion and Future Work:

In summary, we have created and examined a capacitive-based force sensor that utilizes ABS material. The sensor is sensitive to force fluctuations, exhibiting a sensitivity of 3 mV/N. It has been assessed for hysteresis, which revealed minimal deviation, highlighting its precision in measuring forces in both incremental and decremental scenarios. The sensor has a resolution of 0.93 N and operates within the

range of 0.93 N to 6.8 N, which is consistent with human finger ranges for different touch gestures, including tapping, pinching, stretching, and sliding on the screen. Regarding its dynamic attributes, the sensor was identified as a second-order system with an underdamped response to step input. The methodology used for dynamic analysis provided crucial insights into its behavior under varying force conditions.

The combined use of Ansys Software for theoretical analysis, practical evaluations of force measurement techniques, and enhancements to signal amplification circuitry has been pivotal in realizing this capacitive-based force sensor using ABS material. This sensor holds potential for diverse applications requiring precise force sensing, and its future applications are eagerly anticipated.

For future enhancements, augmenting the capacitance value by adjusting area or distance to refine variations is recommended. A more detailed exploration of dynamic characteristics and experimentation with various circuit components could further amplify circuit sensitivity.

## X. References


[1] Kisić, Milica and Blaž, Nelu and Živanov, Ljiljana and Damnjanović, Mirjana, 2019 42nd International Spring Seminar on Electronics Technology (ISSE), Capacitive Force Sensor Fabricated in Additive Technology, 2019, 1-5, 10.1109/ISSE.2019.8810154

[2] Bodini, Andrea and Pandini, Stefano and Sardini, Emilio and Serpelloni, Mauro, 2018 IEEE Sensors Applications Symposium (SAS), Design and fabrication of a flexible capacitive coplanar force sensor for biomedical applications, 2018, 1-5, 10.1109/SAS.2018.8336775

[3] Chu, Henry K. and Mills, James K. and Cleghorn, William L., 2007 7th IEEE Conference on Nanotechnology (IEEE NANO), Design of a High Sensitivity Capacitive Force Sensor, 2007, 29-33, 10.1109/NANO.2007.4601134

[4] Kim, Uikyum and Lee, Dong-Hyuk and Kim, Yong Bum and Seok, Dong-Yeop and Choi, Hyouk Ryeol, IEEE/ASME Transactions on Mechatronics, A Novel Six-Axis Force/Torque Sensor for Robotic Applications, 2017, 22, 3, 1381-1391, 10.1109/TMECH.2016.2640194

[5] Fu, Liyue and Song, Aiguo, IEEE Access, Model-Based Load Characteristics Analysis of the Multi-Dimensional Force Sensor, 2020, 8, 116431-116440, 10.1109/ACCESS.2020.3004113

[6] Fu, Liyue, and Aiguo Song. ”Model-based load characteristics analysis of the multi-dimensional force sensor.” IEEE Access 8 (2020): 116431-116440.

[7] Osoinach, Bryce. ”Proximity capacitive sensor technology for touch sensing applications.” Freescale White Paper 12 (2007): 1-12.